

The SPARC Data Initiative: comparisons of CFC-11, CFC-12, HF and SF6 climatologies from international satellite limb sounders

Article

Published Version

Creative Commons: Attribution 3.0 (CC-BY)

Tegtmeier, S., Hegglin, M. I. ORCID: <https://orcid.org/0000-0003-2820-9044>, Anderson, J., Funke, B., Gille, J., Jones, A., Smith, L., von Clarmann, T. and Walker, K. A. (2016) The SPARC Data Initiative: comparisons of CFC-11, CFC-12, HF and SF6 climatologies from international satellite limb sounders. *Earth System Science Data*, 8 (1). pp. 61-78. ISSN 1866-3516 doi: 10.5194/essd-8-61-2016 Available at <https://centaur.reading.ac.uk/62256/>

It is advisable to refer to the publisher's version if you intend to cite from the work. See [Guidance on citing](#).

Published version at: <http://www.earth-syst-sci-data.net/8/61/2016/essd-8-61-2016.pdf>

To link to this article DOI: <http://dx.doi.org/10.5194/essd-8-61-2016>

Publisher: Copernicus Publications

the [End User Agreement](#).

www.reading.ac.uk/centaur

CentAUR

Central Archive at the University of Reading

Reading's research outputs online



The SPARC Data Initiative: comparisons of CFC-11, CFC-12, HF and SF₆ climatologies from international satellite limb sounders

S. Tegtmeier¹, M. I. Hegglin², J. Anderson³, B. Funke⁴, J. Gille^{5,6}, A. Jones^{7,a}, L. Smith⁶,
T. von Clarmann⁸, and K. A. Walker⁷

¹GEOMAR Helmholtz Centre for Ocean Research Kiel, Ocean Circulation and Climate Dynamics, Kiel,
Germany

²University of Reading, Department of Meteorology, Reading, UK

³Hampton University, Atmospheric and Planetary Sciences, Hampton, Virginia, USA

⁴Instituto de Astrofísica de Andalucía, CSIC, Solar system Department, Granada, Spain

⁵University of Colorado, Atmospheric and Oceanic Sciences, Boulder, Colorado, USA

⁶National Center for Atmospheric Research, Atmospheric Chemistry Observations and Modeling, Boulder,
Colorado, USA

⁷University of Toronto, Department of Physics, Toronto, Ontario, Canada

⁸Karlsruhe Institute of Technology, Institute for Meteorology and Climate Research, Karlsruhe, Germany

^anow at: Chalmers University, Earth and Space Sciences, Göteborg, Sweden

Correspondence to: S. Tegtmeier (stegtmeier@geomar.de)

Received: 2 February 2015 – Published in Earth Syst. Sci. Data Discuss.: 29 September 2015

Revised: 4 January 2016 – Accepted: 9 January 2016 – Published: 11 February 2016

Abstract. A quality assessment of the CFC-11 (CCl₃F), CFC-12 (CCl₂F₂), HF, and SF₆ products from limb-viewing satellite instruments is provided by means of a detailed intercomparison. The climatologies in the form of monthly zonal mean time series are obtained from HALOE, MIPAS, ACE-FTS, and HIRDLS within the time period 1991–2010. The intercomparisons focus on the mean biases of the monthly and annual zonal mean fields and aim to identify their vertical, latitudinal and temporal structure. The CFC evaluations (based on MIPAS, ACE-FTS and HIRDLS) reveal that the uncertainty in our knowledge of the atmospheric CFC-11 and CFC-12 mean state, as given by satellite data sets, is smallest in the tropics and mid-latitudes at altitudes below 50 and 20 hPa, respectively, with a 1σ multi-instrument spread of up to $\pm 5\%$. For HF, the situation is reversed. The two available data sets (HALOE and ACE-FTS) agree well above 100 hPa, with a spread in this region of ± 5 to $\pm 10\%$, while at altitudes below 100 hPa the HF annual mean state is less well known, with a spread $\pm 30\%$ and larger. The atmospheric SF₆ annual mean states derived from two satellite data sets (MIPAS and ACE-FTS) show only very small differences with a spread of less than $\pm 5\%$ and often below $\pm 2.5\%$. While the overall agreement among the climatological data sets is very good for large parts of the upper troposphere and lower stratosphere (CFCs, SF₆) or middle stratosphere (HF), individual discrepancies have been identified. Pronounced deviations between the instrument climatologies exist for particular atmospheric regions which differ from gas to gas. Notable features are differently shaped isopleths in the subtropics, deviations in the vertical gradients in the lower stratosphere and in the meridional gradients in the upper troposphere, and inconsistencies in the seasonal cycle. Additionally, long-term drifts between the instruments have been identified for the CFC-11 and CFC-12 time series. The evaluations as a whole provide guidance on what data sets are the most reliable for applications such as studies of atmospheric transport and variability, model–measurement comparisons and detection of long-term trends. The data sets will be publicly available from the SPARC Data Centre and through PANGAEA (doi:10.1594/PANGAEA.849223).

1 Introduction

Trichlorofluoromethane (CCl_3F ; herein referred to by its common name, CFC-11) and dichlorodifluoromethane (CCl_2F_2 ; herein CFC-12) belong to the chlorofluorocarbons (CFCs), which are an important group of the chlorine-containing ozone-depleting substances. CFC-11 and CFC-12 are anthropogenic compounds with virtually no natural background and were emitted by human activity through their wide use as refrigerants, for foam blowing and as aerosol spray propellants (Montzka and Reimann, 2011, and references therein). Both anthropogenic source gases are distributed and accumulated in the troposphere before being transported into the stratosphere, where they are converted into reactive halogens which cause severe ozone depletion (Molina and Rowland, 1974). Complying with the Montreal Protocol in the late 1980s and its amendments and adjustments, their manufacture was banned in many countries due to their damage to the ozone layer. Consequently, global CFC-11 surface mixing ratios peaked in the mid-1990s and are now slowly decreasing as reported by three independent sampling networks (Montzka and Reimann, 2011). Accordingly, a decrease in the total atmospheric burden of the long-lived CFC-11, with an atmospheric lifetime of 52 years, has been observed based on ground-based total-column measurements at the Jungfraujoch station (Zander et al., 2005; Montzka and Reimann, 2011). Global CFC-12 abundance reached a peak in 2000–2004 (Montzka and Reimann, 2011) and shows a delayed decline compared to CFC-11 due to its long lifetime (102 years) and continuing emissions from CFC-12 banks, namely, thermal insulating foams as well as refrigeration and air conditioning equipment (Daniel et al., 2007).

In addition to in situ (e.g., Bujok et al., 2001), air-sampling (Engel et al., 1998) and remote infrared spectroscopy (e.g., Johnson et al., 1995; Toon et al., 1999) measurement techniques, stratospheric CFC-11 and CFC-12 have been measured by multiple satellite-borne solar occultation and limb-emission instruments. Most important, vertically resolved CFC-11 and CFC-12 measurements are from MIPAS (Hoffmann et al., 2008; Kellmann et al., 2012), ACE-FTS (Mahieu et al., 2008; Brown et al., 2011), and HIRDLS (Gille et al., 2013). While ACE-FTS and MIPAS both show declining mixing ratios in the upper troposphere and lower stratosphere (UTLS) region consistent with surface observations, CFC-11 and CFC-12 trends in the middle stratosphere derived from MIPAS measurements change with latitude and can even be positive in some regions (Kellmann et al., 2012). A thorough assessment of the degree to which the three data sets agree with each other is critical in order to analyze the consistency in trends derived from these platforms and from surface data.

Hydrogen fluoride (HF) is primarily produced through the photodissociation of anthropogenic CFCs and hydrochloro-

rofluorocarbons (HCFCs) (e.g., Luo et al., 1995). Once produced, HF is the dominant reservoir of fluorine atoms and has a stratospheric lifetime on the order of more than 10 years, during which it accumulates in the stratosphere (Molina and Rowland, 1974; Stolarski and Rundel, 1975). The removal of HF happens through downward transport into the troposphere and subsequent rainout or by upward transport to the mesosphere, where it is destroyed by photolysis. Since HF is a direct product of CFCs and HCFCs it is considered a useful tracer for monitoring anthropogenic changes in the stratospheric composition. Various measurement systems, including surface in situ and ground-based, airborne and balloon-borne Fourier transform infrared spectroscopy measurements (FTIR), have reported a rapid increase in HF over the last decades (e.g., Kohlhepp et al., 2012). A comparison of spaceborne FTIR measurements from ATMOS in 1985 and 1994 and solar occultation measurements from ACE-FTS in 2004 indicates a slowing-down of the HF increase over this time period (Rinsland et al., 2005). In addition to ACE-FTS, near-global satellite measurements of HF are available from HALOE for the time period 1991–2005 with an overlap of the two data sets for 2004–2005. In order to estimate long-term changes in HF over the last two decades, a thorough comparison of HALOE and ACE-FTS measurements, as carried out in this study, is necessary. Due to its long lifetime, HF can also be used as a tracer of transport of air masses with the Brewer–Dobson circulation (BDC) and for separating dynamics and chemistry in polar regions (e.g., Luo et al., 1995).

Another gas often used as a tracer for transport with the BDC is sulfur hexafluoride (SF_6). It is of tropospheric origin and mainly employed in large electrical equipment, from where it escapes into the atmosphere through leakage and venting during maintenance (Ko et al., 1993). Once in the atmosphere it absorbs infrared radiation, and it is one of the most efficient greenhouse gases known at this time, with a greenhouse effect of 23 900 times that of CO_2 . SF_6 is chemically inert in the troposphere and stratosphere and is only removed through transport into the mesosphere, where it is destroyed by photolysis or electron capture reactions (Morris et al., 1995; Reddmann et al., 2001). As a result, it has an atmospheric lifetime of hundreds to thousands of years (Ko et al., 1993; Ravishankara et al., 1993). Growing anthropogenic SF_6 emissions over the last decades have led to its increase in the atmosphere (Levin et al., 2010). This, in combination with its long lifetime, makes SF_6 a suitable tracer to derive estimates of the mean age of stratospheric air (Hall and Plumb, 1994; Volk et al., 1997), which is a good measure of the strength of the BDC (Austin and Li, 2006). Due to recent model predictions of an intensified BDC (Butchart et al., 2006), observational evidence of the long-term changes in age of air is a focus of ongoing research (e.g., Stiller et al., 2012; Haenel et al., 2015). Stratospheric SF_6

Table 1. Full instrument name, satellite platform, measurement mode, and wavelength category of all instruments included in this study given in order of satellite launch date.

| Instrument | Full name | Satellite platform | Measurement mode | Wavelength category |
|------------|---|--------------------|-------------------|---------------------|
| HALOE | The Halogen Occultation Experiment | UARS | Solar occultation | Mid-infrared |
| MIPAS | Michelson Interferometer for Passive Atmospheric Sounding | Envisat | Emission | Mid-infrared |
| ACE-FTS | Atmospheric Chemistry Experiment – Fourier Transform Spectrometer | SCISAT-1 | Solar occultation | Mid-infrared |
| HIRDLS | High Resolution Dynamics Limb Sounder | Aura | Emission | Mid-infrared |

data are available from aircraft measurements in the 1990s (Elkins et al., 1996), from balloon-borne and airborne profile measurements (e.g., Volk et al., 1997; Engel et al., 2006) and from ATMOS measurements onboard the ATLAS space shuttle (e.g., Rinsland et al., 1993). First continuous near-global satellite measurements have been made by MIPAS (Stiller et al., 2008) and ACE-FTS (Brown et al., 2011).

The first comprehensive intercomparison of CFC-11, CFC-12, HF, and SF₆ data products available from limb-viewing satellite instruments was performed as part of the Stratosphere-troposphere Processes And their Role in Climate (SPARC) Data Initiative (SPARC Data Initiative Report, 2016) and is presented in this paper. The new concept of satellite measurement validation presented here is based on a “top-down” approach comparing all available satellite data sets and thus providing a global picture of the data characteristics. The comparisons will provide basic information on quality and consistency of the various data sets and will serve as a guide for their use in empirical studies of climate and variability, and in model–measurement comparisons. For each gas, the spread in the climatologies is used to provide an estimate of the overall systematic uncertainty in our knowledge of the atmospheric mean state derived from satellite data sets. Such an assessment of the relative uncertainty yields information on how well we know the global annual mean distribution of each gas and will help to identify regions where more detailed evaluations or more data are needed. The few cases where independent measurements suggest that the satellite-derived uncertainty could be only a lower-bound estimate are discussed.

The individual monthly zonal mean time series are compared in terms of their zonal mean climatologies to identify mean biases between the instruments and their latitudinal and vertical structure. In addition to the spatial structure of the deviations between the data sets, it is of interest to analyze the temporal variations in the differences in terms of seasonal, interannual and long-term changes. Data sets and methods are described in Sect. 2. The evaluations of the four gases (CFC-11, CFC-12, HF and SF₆) can be found in Sects. 3 to 6 and the summary is given in Sect. 7. The trace gas comparisons presented here are part of a larger project (SPARC Data Initiative) which compares 25 different chem-

ical tracers, including ozone (Tegtmeier et al., 2013; Neu et al., 2014), water vapor (Hegglin et al., 2013) and aerosol climatologies from international satellite limb sounders.

2 Data and methods

2.1 Satellite instruments and climatologies

CFC-11, CFC-12, HF, and SF₆ data products with a high vertical resolution from limb-viewing satellite instruments are the focus of this study. Limb-viewing sounders measure trace gas signals by looking horizontally through the atmosphere, which allows the retrieval of stratospheric gases with low concentrations (due to the long atmospheric ray path) at a high vertical resolution (due to variations in the observation angle). These measurements extend from the mid-troposphere to as high as the mesosphere. The instruments participating in this study are given with their full instrument name, satellite platform, measurement mode, and wavelength category in Table 1. Detailed information on the individual instruments, including their sampling patterns and retrieval techniques, can be found in the SPARC Data Initiative report.

The trace gas climatologies from the individual satellite instruments consist of zonal monthly mean time series calculated on the SPARC Data Initiative climatology grid using 5° latitude bins and 28 pressure levels. Note that the term climatology within the SPARC Data Initiative is not used to refer to a time-averaged climate state (which should be reproduced by free-running models, averaged over many years) but rather to refer to year-by-year values (which free-running models would not be expected to match). The zonal monthly mean volume mixing ratio (VMR) and the standard deviation along with the number of averaged data values are given for each month, latitude bin, and pressure level. Furthermore, the mean, minimum, and maximum local solar time; the average latitude; and the average day of the month within each bin for one selected pressure level are provided. The time series of all variables are saved in a consistent netcdf format and will be publicly available from the SPARC Data Centre (<http://www.sparc-climate.org/data-center/>). Note that while the SPARC Data Initiative is an ongoing activity, the data sets presented here include measurements until the end of 2010.

Table 2. Data version, time period, vertical range and resolution, and validation references for the CFC-11, CFC-12, HF, and SF₆ data sets included in this study.

| | Instrument and data version | Time period | Vertical range | Vertical resolution | References |
|-----------------|-----------------------------|----------------------|----------------|---------------------|-----------------------------|
| CFC-11/ CFC-12 | MIPAS 10 | Mar 2002 to Mar 2004 | 10–35/50 km | 4 km | Kellmann et al. (2012) |
| | MIPAS 220 | Jan 2005 to Apr 2012 | | | |
| | ACE-FTS V2.2 | Mar 2004 to Dec 2010 | 5/6–22/28 km | 3–4 km | Mahieu et al. (2008) |
| | HIRDLS V7.0 | Jan 2005 to Mar 2008 | 10–24/30 km | 1 km | Gille et al. (2013) |
| HF | HALOE V19 | Oct 1991 to Nov 2005 | 12–65 km | 3.5 km | Groß and Russell III (2005) |
| | ACE-FTS V2.2 | Mar 2004 to Apr 2012 | 12–55 km | 3–4 km | Mahieu et al. (2008) |
| SF ₆ | MIPAS 201 | Jan 2005 to Apr 2012 | 6–50 km | 4–6 km | Stiller et al. (2008) |
| | ACE-FTS V2.2 | Mar 2004 to Dec 2010 | 6–35 km | 3–4 km | Brown et al. (2011) |

Updates of the climatologies including additional years after 2010 will be made available in the future.

The climatology construction follows a common methodology described below. First, the original data products are carefully screened according to recommendations given in relevant quality documents, in published literature, or according to the best knowledge of the instrument scientists involved. For HALOE, each individual profile is first screened for clouds and heavy aerosols. For MIPAS, measurements affected by clouds are discarded from the analysis, and results where the diagonal element of the averaging kernel is below a given threshold are excluded, as well as results from non-converged retrievals. For ACE-FTS, data are excluded if the fitting uncertainty value is 100 % of its corresponding VMR value and where a given uncertainty value is 0.01 % of its corresponding VMR value. The binned ACE-FTS data are subject to statistical analysis and observations larger than three median absolute deviations (MADs) from the median value in each grid cell are disregarded. For HIRDLS, a processor creates statistically best estimates based on a time series Kalman filter analysis. Parameter choice during the analysis and spike detection based on level 2 uncertainties limit the range of the data to physically reasonable values.

In a second step, the data products are interpolated to a common pressure grid (300, 250, 200, 170, 150, 130, 115, 100, 90, 80, 70, 50, 30, 20, 15, 10, 7, 5, 3, 2, 1.5, 1, 0.7, 0.5, 0.3, 0.2, 0.15, and 0.1 hPa) using a linear interpolation in log pressure, except for ACE-FTS, where individual measurements are vertically binned using the mid-points between the pressure levels (in log pressure) to define the bins. For ACE-FTS, the binning method has been chosen over interpolation in order to stay consistent with the recently published ACE-FTS climatology suite that uses this binning method (Jones et al., 2011, 2012). For MIPAS and ACE-FTS, a conversion from altitude to pressure levels is performed using retrieved temperature–pressure profiles. Zonal monthly mean products for 36 latitude bins (with mid-points at 87.5° S, 82.5° S, ... 87.5° N) are calculated as the average of all of properly screened measurements on a given pressure level within each

latitude bin and month. For most instruments, a minimum of five measurements within the bin is required to calculate a monthly zonal mean. Sample sizes within each monthly latitude bin vary with the measurement type and instrument, and range from 5–200 measurements per bin (ACE-FTS) to >2000 measurements per bin (HIRDLS) (see Toohey et al., 2013, Fig. 1). Detailed information on the climatology construction including the screening process for each individual instrument can be found in the SPARC Data Initiative report. For each data set, the data version, time period, vertical range, and resolution, as well as relevant references, are given in Table 2. Note that for 2002–2004, MIPAS operated in full spectral resolution, while for 2005–2010 MIPAS operated in reduced spectral resolution. Full version numbers for MIPAS 2002–2004 data are V3O_CFC11_10, and V3O_CFC12_10, and for MIPAS 2005–2010 data are V5R_CFC11_220, V5R_CFC12_220, and V5R_SF6_201.

2.2 Climatology diagnostics and uncertainties

This study aims at analyzing the mean differences between the various data sets based on a set of standard diagnostics including the comparison of annual and monthly zonal mean climatologies averaged over a maximum number of years. We will apply the multi-instrument mean (MIM) throughout this study as a common point of reference. The MIM is calculated as the mean over the monthly zonal mean time series from all available instruments within a given time period of interest. It should be clarified that the MIM is not a data product and will not be provided together with the instrument climatologies. By no means is the choice of the MIM based on the assumption that the MIM is the best estimate of the atmospheric trace gas field; rather, it is motivated by the need for a reference that does not favor a certain instrument. Note that the MIM has a number of shortcomings including the fact that the composition of instruments from which the MIM is calculated can change between different time periods and regions.

The evaluation of the multi-year annual mean climatologies aims to identify mean biases between the instruments

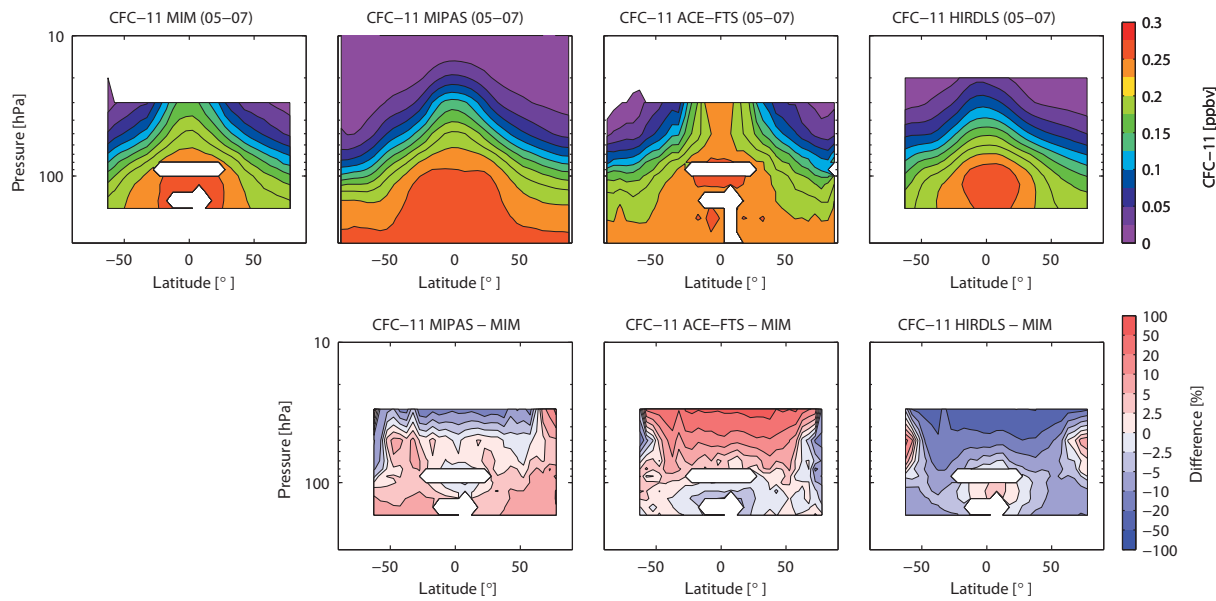


Figure 1. Altitude–latitude cross sections of annual zonal mean CFC-11 for the MIM, MIPAS, ACE-FTS and HIRDLS (upper panels) and relative differences between the individual instruments and the MIM (lower panels) are shown for 2005–2007.

Table 3. Definitions and abbreviations of different atmospheric regions used for the evaluations.

| Region | Abbreviation | Lower boundary | Upper boundary |
|---------------------|--------------|----------------|----------------|
| Upper troposphere | UT | 300 hPa | Tropopause |
| Lower stratosphere | LS | Tropopause | 30 hPa |
| Middle stratosphere | MS | 30 hPa | 5 hPa |
| Upper stratosphere | US | 5 hPa | 1 hPa |
| Lower mesosphere | LM | 1 hPa | 0.1 hPa |

and their latitudinal and vertical structure. The notations for different atmospheric regions used throughout the evaluations are given in Table 3. Relative differences between an instrumental climatology and the MIM are calculated as the absolute difference between the two divided by the MIM. In addition to the spatial structure of the deviations between the data sets, it is of interest to analyze the temporal variations in the differences in terms of seasonal, interannual, and long-term changes. The latter is based on a drift analysis, identifying linear, long-term changes in the difference time series between two instruments. For this purpose, the difference time series for every latitude bin and pressure level are calculated and analyzed with a multi-linear regression model including a constant and a linear term as well as several harmonic functions (von Clarmann et al., 2010; Eckert et al., 2014). The number and period length of the harmonic functions depend on the data sets analyzed and are given in the relevant evaluation subsection.

Monthly zonal mean trace gas climatologies can differ from the true mean atmospheric state due to random and systematic errors in the measurements. For solar occultation in-

struments like ACE-FTS and HALOE (5–200 measurements per bin), low sample sizes can be symptomatic of random errors, due to simple undersampling of the measured population. Low sample sizes are also often associated with nonuniform spatiotemporal sampling (e.g., measuring only at the beginning or end of a month), which can lead to large random or systematic errors in the climatologies (Toohey et al., 2013). In addition, changes in the latitudinal coverage from month to month, which are frequent for solar occultation instruments, can lead to latitudinal discontinuities in annual means. Such characteristics have been shown for ACE-FTS and HALOE sampling biases identified in the annual mean ozone field in Toohey et al. (2013). An approximate measure of the impact of random errors on the mean value due to simple undersampling of the measured population is given by the standard error of the mean (SEM), calculated from n measurements with a standard deviation (SD) as $SEM = SD/\sqrt{n}$. Note that the SEM can be an over- or underestimate of the true uncertainty in the mean (Toohey and von Clarmann, 2013) since satellite sampling patterns can be quite different than the random sampling assumed in the formulation of the SEM. Despite this shortcoming, due to its frequent use in past studies, the SEM will be used as an approximate measure of uncertainty in each individual climatological mean, graphically illustrated by $2 \times SEM$ error bars, which can be interpreted as a 95 % confidence interval of the mean (under the assumption that the measurements are normally distributed).

However, it should be stressed that this statistical error in the mean is in many cases much smaller than the overall error of the climatology, which contains the systematic errors

of both the measurements and the climatology construction, e.g., due to instrument sampling (Toohey et al., 2013) and different averaging techniques (Funke and von Clarmann, 2012). A complete characterization of the systematic errors would require a precise knowledge of the absolute measurement uncertainties including a range of error sources such as uncertainty in the spectroscopic data, calibration, pointing accuracy, and others. Such knowledge is not available derived in a consistent way according to a common standard for all instruments. In the absence of such bottom-up measurement uncertainties, we will use the inter-instrument spread of climatologies as a measure of the uncertainty in the underlying trace gas field. Information from other in situ, ground- or balloon-based remote measurements cannot be included in the uncertainty estimates in a systematic way due to their sparseness. The few cases where validation studies suggest that the satellite-derived uncertainty could be only a lower estimate (i.e., differences to in situ measurements are larger than among the satellite data sets) are discussed.

3 Evaluation of the CFC-11 climatologies

3.1 Spatial structure of the differences

The annual zonal mean CFC-11 climatologies for MIPAS, ACE-FTS, HIRDLS and their MIM for the maximum overlap period of the three instruments (2005–2007) are shown in Fig. 1 (upper panel). The maximum CFC-11 mixing ratios are found in the troposphere and in the tropical tropopause layer (TTL), where air is entrained from the troposphere into the stratosphere. For MIPAS and HIRDLS, these maximum mixing ratios in the TTL are partially larger (up to 0.275 ppbv) than those inferred from surface measurements (0.26 ppbv; Eckert et al., 2015), suggesting a local bias of up to 5 %. These discrepancies represent so far unexplained problems in the satellite data sets and dedicated, instrument-specific validation studies are required in order to explain them. Overall, MIPAS shows the largest mixing ratios in the TTL with a very flat isoline at 100 hPa extending from 30° S to 30° N and a uniform distribution at altitudes below. Due to the long CFC-11 lifetime, such a uniform distribution in the TTL is expected in contrast to the local maximum in the upper TTL as seen in the ACE-FTS or HIRDLS climatologies. For ACE-FTS, mixing ratios increase from 0.24 ppb in the troposphere to 0.26 ppb at the tropopause, and for HIRDLS the values increase from 0.25 to 0.27 ppb. Above the tropopause, CFC-11 decreases rapidly with isolines roughly parallel to the north-south slope of the tropopause for MIPAS. HIRDLS shows some unrealistically steep gradients at altitudes below 70 hPa, in particular in the Southern Hemisphere (SH). Additional evaluations (not shown) revealed that these steep vertical gradients are also present if the vertical resolution of the HIRDLS climatology is reduced to match the MIPAS or ACE-FTS resolution, and are therefore in all likelihood not related to resolution as-

pects. In the tropics, CFC-11 from the ACE-FTS climatology does not decrease between 50 and 30 hPa and therefore the isolines in the inner tropics look quite different compared to the two other instruments. This might be related to the retrieval having a fixed altitude limit at all latitudes (rather than extending to higher altitudes in the tropics) impacting the highest ACE-FTS levels in the climatology. Also, the ACE-FTS sampling in the tropics is much lower than HIRDLS and MIPAS sampling.

Differences of the individual data sets to the MIM are also shown in Fig. 1 (lower panel). The instruments agree well at altitudes below 100 hPa with differences to the MIM up to $\pm 10\%$, with MIPAS on the high side, HIRDLS on the low side and ACE-FTS in the middle, except for the tropics, where ACE-FTS is lowest. Above the tropopause, the relative differences increase slowly as the absolute CFC-11 abundance decreases. In the tropics above 50 hPa, there are large discrepancies between ACE-FTS and HIRDLS with differences to the MIM of up to +50 and -50% , respectively. MIPAS is mostly in the middle range and at the highest altitudes somewhat closer to HIRDLS. Note that HIRDLS shows much higher values in the high-latitude middle stratosphere than the other two data sets. Evaluations of the monthly mean climatologies (see Supplement Figs. S1–S4 for January, April, July and October) are overall consistent with the annual mean comparisons.

Figure 2a displays the latitudinal structure of the relative differences, as an example, for the month of August at 50 and 170 hPa. Notable features at 50 hPa are the large differences in the tropics and the reduced absolute differences in the mid-latitudes, also apparent in the differently shaped ACE-FTS isolines mentioned earlier. At 170 hPa, the latitudinal gradients of all three data sets show considerable differences ranging from very steep gradients for HIRDLS to relatively flat gradients for MIPAS. The largest differences can be observed in the respective winter hemisphere high latitudes, a characteristic which is confirmed by further monthly mean evaluations for Northern Hemisphere (NH) winter (not shown here).

Figure 2b shows vertical CFC-11 profiles for latitude bands and months where comparisons with balloon-borne measurements are available (35–40° N in August, 65–70° N in January) from individual satellite validation studies (Mahieu et al., 2008). In the mid-latitudes, the monthly mean comparison confirms the outcome of the annual mean evaluations (Fig. 1), where HIRDLS is considerably lower than the other two instruments with differences to the MIM of -5% (at altitudes below 100 hPa) to -40% (at 20 hPa). ACE-FTS and MIPAS, on the other hand, are closer together with differences of around $\pm 2.5\%$ at altitudes below 70 hPa and positive deviations of +20 % above 70 hPa. Balloon-borne measurements of the Jet Propulsion Laboratory (JPL) Mark-IV Interferometer (Toon et al., 1999) for September 2003–2005 at 35° N have been compared to ACE-FTS zonal mean values over 30–40° N for August–October 2004–2006 by Mahieu

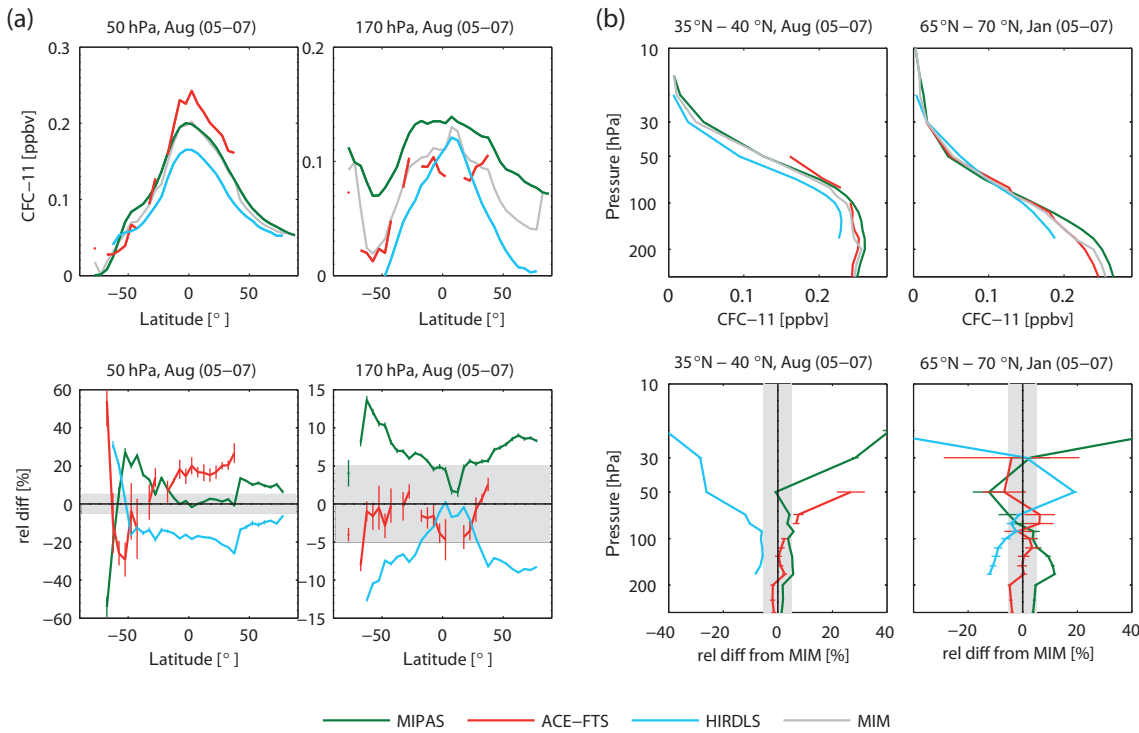


Figure 2. Meridional monthly zonal mean CFC-11 profiles at 50 and 170 hPa for August 2005–2007 (upper row) and relative differences between the individual instruments and the MIM profiles (lower row) are shown in panel (a). Vertical monthly zonal mean CFC-11 profiles for 35–40° N in August and 65–70° N in January 2005–2007 (upper row) and relative differences between the individual instruments and the MIM profiles (lower row) are shown in panel (b). The grey shading indicates the $\pm 5\%$ difference range. Bars indicate the uncertainties in the relative differences.

et al. (2008). The comparison shows good agreement with slightly lower (up to -10%) satellite measurements at altitudes below 100 hPa. Consequently, mid-latitude HIRDLS data likely have a low bias at all altitudes. MIPAS data are closest to the balloon-borne measurements at altitudes below 70 hPa, while above this level the relatively high ACE-FTS mixing ratios are confirmed. Note, however, that these conclusions are based on a comparison of zonal mean satellite data with individual balloon-borne profiles.

At high latitudes (right panels in Fig. 2b) between 50 and 30 hPa, HIRDLS reveals positive deviations with respect to the MIM in contrast to all other latitudes. The monthly mean ACE-FTS data are mostly in the middle between the two other instruments, which is not in agreement with the evaluations of the annual mean profiles, showing strong negative deviations. Such disagreement indicates that at high latitudes the annual mean ACE-FTS field is not representative of a mean based on all 12 months due to the sparse sampling of the solar occultation instrument. Coincident profiles from the balloon-borne limb-sounding observations of the Far-Infrared Spectrometer (FIRS)-2 (Johnson et al., 1995) in January 2007 at 68°N show 10 to 40 % larger values than ACE-FTS (Mahieu et al., 2008). If one assumes similar differences between the two systems for the complete

latitude band, then this would place the balloon-borne observations right in between the ACE-FTS and MIPAS profile for the region below 100 hPa. However, above 100 hPa, the balloon-borne measurements reveal relatively large CFC-11 mixing ratios resulting in positive deviations of $+40\%$ with respect to MIPAS and ACE-FTS and a good agreement with HIRDLS, which also deviates significantly from MIPAS and ACE-FTS. Such differences could be, among other things, caused by the different vertical resolutions of the instruments.

3.2 Temporal variations in the differences

Seasonal and interannual variability of CFC-11 is dominated by the quasi-biennial oscillation (QBO) signal in the tropical MS and by the annual cycle at high latitudes (e.g., Kellmann et al., 2012). In the tropics (Supplement Fig. S5), MIPAS shows a very clear QBO cycle and the other two data sets seem to also display the signal, although due to the shortness of the HIRDLS time series (3 years) and the frequent data gaps in ACE-FTS an unambiguous conclusion is not possible. The annual cycle at high latitudes, caused by descent of aged air in the winter polar vortex, is captured by all three data sets in the NH (Supplement Fig. S6), while in the SH, ACE-FTS does not detect the same annual variations (Sup-

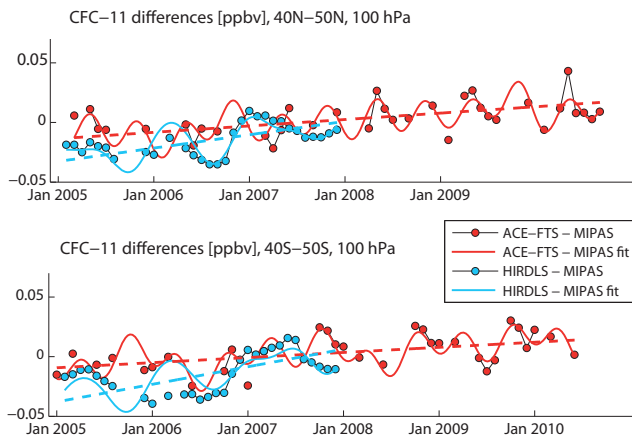


Figure 3. Time series of zonal monthly mean CFC-11 absolute differences between ACE-FTS and MIPAS (black lines, red symbols) as well as HIRDLS and MIPAS (black lines, blue symbols) are given for 2005 to 2010 at 40–50° N and 40–50° S at 100 hPa. Additionally, the calculated fit (solid colored line) and the corresponding linear term (dashed colored line) are shown.

plement Fig. S7). The impact of the sampling patterns on the monthly zonal mean values provided by solar occultation instruments in the case of a distorted polar vortex have been shown to be about 10–20 % for ozone fields (Toohey et al., 2013) and are, therefore, very likely not responsible for the 50–100 % larger CFC-11 values reported by ACE-FTS during SH winter. Note that the SH high-latitude differences do not show up in the annual mean comparisons, which are limited to regions where all three data sets overlap (60° S–80° N).

In addition to different seasonal and interannual variations, the data sets can also differ in their long-term changes. Such differences would be of importance for trend studies and are investigated here by a multi-linear regression analysis of the time series of differences between pairs of instruments. As an example, Fig. 3 shows the absolute differences of both ACE-FTS and HIRDLS with respect to MIPAS at 100 hPa for 40–50° S and 40–50° N. Also displayed are the fits of these difference time series based on a multi-linear regression with six harmonic functions for ACE-FTS (period length 6, 8, 9, 12, 18, and 24 months) and four harmonic functions for HIRDLS (period length 6, 8, 9, and 12). The linear terms of the fits of the difference time series are not zero, indicating possible drifts between the instruments. In both hemispheres, ACE-FTS and HIRDLS show a positive trend of their differences with respect to MIPAS, with the differences increasing over time. Note that, for HIRDLS, only 3 years of data are available and thus the linear fit term of the HIRDLS differences with respect to MIPAS estimated for this time period could also be related to a different representation of some multi-year oscillation (e.g., the QBO signal) in the different climatologies.

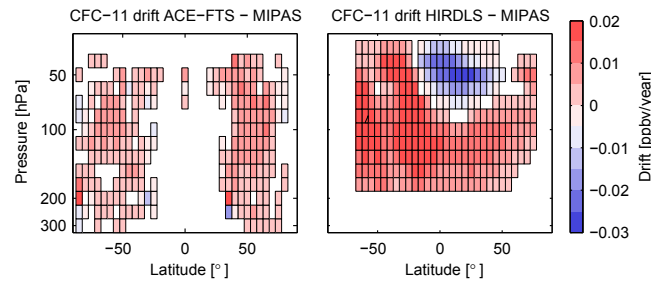


Figure 4. Altitude–latitude cross sections of drifts between ACE-FTS and MIPAS (left panel) and HIRDLS and MIPAS (right panel) CFC-11 climatologies are given in the form of the linear terms $[\text{ppbv year}^{-1}]$ derived from multi-linear regression of the difference time series.

Hereinafter, we will refer to the linear term $[\text{ppbv year}^{-1}]$ derived from the regression of the time series of differences between pairs of instruments as the “drift” term. Figure 4 shows the altitude–latitude cross section of drifts between ACE-FTS and MIPAS (left panel) and HIRDLS and MIPAS (right panel) CFC-11 climatologies. Only significant linear trend terms (with $p < 0.05$ assuming normally distributed uncorrelated residuals) based on difference time series with more than 15 data points are displayed. Both ACE-FTS and HIRDLS show mostly positive drifts with respect to MIPAS of up to $0.02 \text{ ppbv year}^{-1}$. For ACE-FTS, positive drifts of the same magnitude are found in the SH and NH mid-latitudes, resulting in a consistent picture with increasing differences everywhere, except for the tropics, where no significant linear changes have been identified. For HIRDLS, the drift terms are slightly larger than for ACE-FTS in particular in the SH. In the tropical LS, HIRDLS shows a negative drift with respect to MIPAS which is not in agreement with the ACE-FTS evaluations. Note that in the tropical UTLS, no drift between ACE-FTS and MIPAS has been identified and that MIPAS trends here have been shown to agree well with tropospheric CFC-11 trends from the Halocarbons and other Atmospheric Trace Species (HATS) group from NOAA (Kellmann et al., 2012).

The drift analysis is based on climatologies instead of coincident single measurements and can therefore contain artifacts resulting from such issues as changes in geospatial sampling with time or differences in instrumental averaging kernels. In the case of long-term changes in sampling, spatial inhomogeneities in the measured trace gas may be mapped into a drift in the climatology. In the case where the atmosphere is subject to altitude-dependent trends, instruments with different vertical resolutions may show different trends at specific heights, which can introduce additional drift effects. Nevertheless, if such artifacts are present in the climatologies, they may impact not only the drift analysis presented above but also the trends based on the monthly zonal mean time series. Therefore, the here-derived drifts provide important

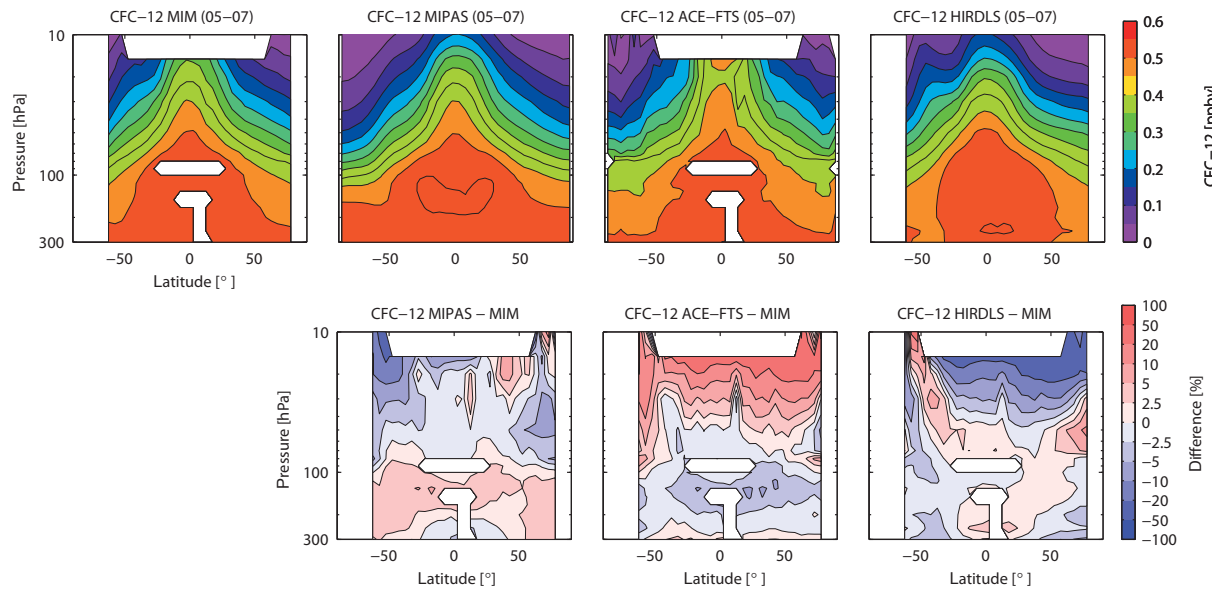


Figure 5. Altitude–latitude cross sections of annual zonal mean CFC-12 for the MIM, MIPAS, ACE-FTS and HIRDLS (upper panels) and relative differences between the individual instruments and the MIM (lower panels) are shown for 2005–2007.

background information for the interpretation of long-term changes in the climatologies.

4 Evaluation of the CFC-12 climatologies

4.1 Spatial structure of the differences

Figure 5 shows the annual zonal mean CFC-12 climatologies for 2005–2007 for all available measurements. Maximum CFC-12 values are reported in all three climatologies in the TTL and also for MIPAS in the extratropical UTLS, similar to what has been observed for CFC-11. For MIPAS (0.57 ppbv) and HIRDLS (0.56 ppbv), the tropical mixing ratios exceed maximum surface measurements (0.54 ppbv), indicating a high bias of the two satellite data sets at altitudes below 100 hPa of up to 5 %. ACE-FTS shows elevated values at the highest retrieval level (15 hPa) when compared to the other two data sets. As described earlier, this is possibly related to the imposed maximum retrieval altitude for all latitudes. Additionally, the solar occultation sounder has noisier isolines related to sampling density with some kinks at the 130 hPa level. HIRDLS isolines above 20 hPa reveal some kinks in the SH mid-latitudes which do not match with our knowledge of large-scale atmospheric motion of long-lived tracers, and seem to be related to retrieval artifacts.

The differences of all three data sets with respect to the MIM are displayed in Fig. 5 (lower panels). At altitudes below 50 hPa, the data sets agree very well with differences of less than ± 5 %. While ACE-FTS is on the low side and MIPAS is on the high side, HIRDLS shows sometimes better agreement with the low ACE-FTS values (SH and NH high latitudes) and sometimes with the high MIPAS values

(tropics and NH mid-latitudes). Except for MIPAS, these relatively small differences increase in the LS/MS with altitude. Above 50 hPa, the largest differences of up to ± 50 % exist between HIRDLS (high side) and ACE-FTS (low side) at the highest ACE-FTS retrieval level (15 hPa), very similar to what has been found for CFC-11. MIPAS is mostly in the middle range but somewhat closer to the HIRDLS values. Evaluations of the monthly mean climatologies (see Supplement Figs. S8–S11 for January, April, July and October) are consistent with the annual mean comparisons.

In Fig. 6a (left panels), meridional CFC-12 profiles for August at 50 hPa and their relative differences with respect to the MIM are presented. All three data sets show very similarly shaped isolines and agree very well with differences below ± 5 % except for the high latitudes. At the southern high latitudes, ACE-FTS detects larger CFC-12 abundances than MIPAS. Relative differences decrease with decreasing altitude and are quite small (≤ 2.5 %) in the tropics at 200 hPa (Fig. 6a). Surprisingly, the relative differences at 200 hPa are larger in the winter hemisphere high latitudes, although there is no such strong meridional gradient as observed for the levels above. These differences result from the fact that CFC-12 derived from ACE-FTS and HIRDLS decreases in the poleward direction, while MIPAS values at high latitudes are very similar to the tropical abundances. These contrary characteristics of the meridional gradients at high latitudes are also observed for other months, and often the deviations are most pronounced in the respective winter/spring hemisphere (similar to CFC-11).

Figure 6b shows vertical CFC-12 profiles for latitude bands and months where comparisons with balloon-borne measurements are available (35–40° N in August, 65–

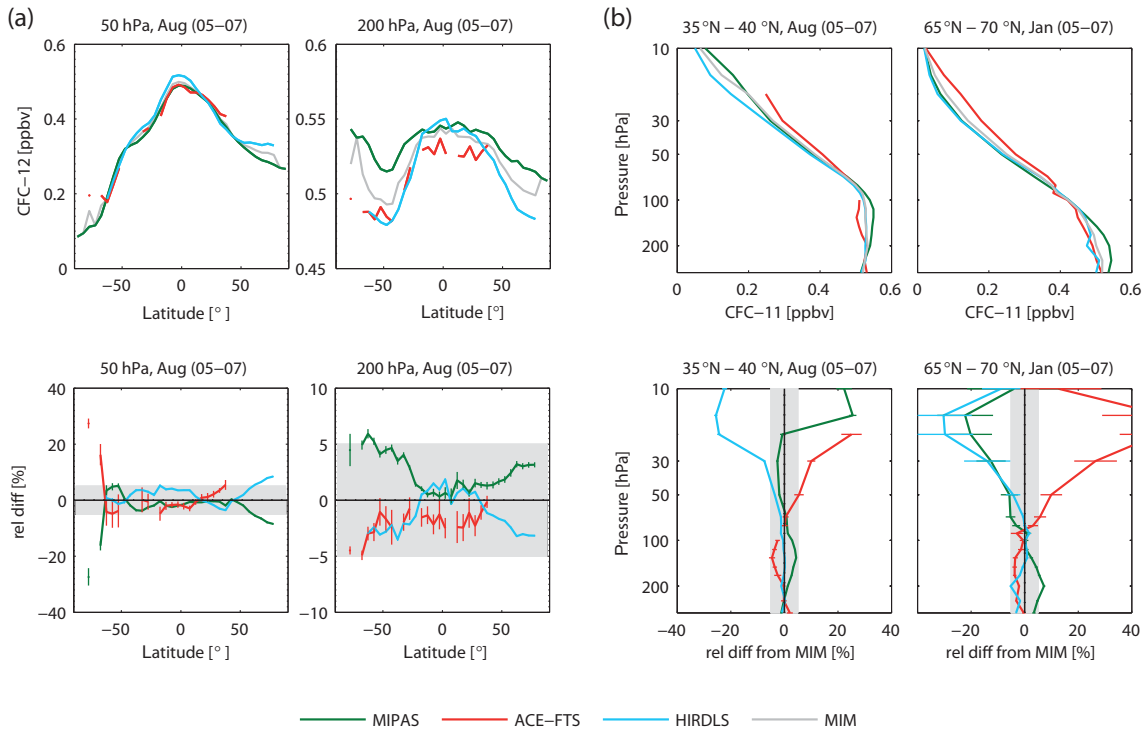


Figure 6. Meridional zonal mean CFC-12 profiles at 50 and 200 hPa for August 2005–2007 (upper row) and relative differences between the individual instruments and the MIM profiles (lower row) are shown in panel (a). Vertical monthly zonal mean CFC-12 profiles for 35–40° N in August and 65–70° N in January 2005–2007 (upper row) and relative differences between the individual instruments and the MIM profiles (lower row) are shown in panel (b). The grey shading indicates the $\pm 5\%$ difference range. Bars indicate the uncertainties in the relative differences.

70° N in January) from individual satellite validation studies (Mahieu et al., 2008). In the mid-latitudes, all three data sets agree well at altitudes below 50 hPa with differences with respect to the MIM of up to $\pm 5\%$, while above 50 hPa differences are large with positive deviations of ACE-FTS of up to +20 % and negative deviations of HIRDLS of up to -20 %. Non-coincident comparison of balloon-borne Mark-IV (Toon et al., 1999) profile measurements (35° N, September 2003–2005) to ACE-FTS zonal mean values (30–40° N, August–October 2004–2006) are presented in Mahieu et al. (2008). The comparison combined with the evaluation of all data sets in Fig. 6b indicates a good agreement of the balloon-borne data with all instruments at altitudes below 100 hPa with smallest deviations to MIPAS. Above 100 hPa, the balloon-borne measurements are larger than all satellite data sets and show the best agreement with ACE-FTS with relatively small differences (5–10 %). As already noted for CFC-11, these conclusions are restricted by the assumption that the evaluation of zonal mean satellite data is consistent with the evaluation of individual balloon profiles.

At high latitudes, the three satellite data sets show similar characteristics when compared to the mid-latitudes. The main differences are higher positive deviations for ACE-FTS (up to +60 % at 20 hPa) and the fact that MIPAS is more

on the low side and therefore closer to HIRDLS. Coincident profiles from the FIRS-2 show 50 % lower values than ACE-FTS at altitudes below 50 hPa (Mahieu et al., 2008). If one assumes similar differences between the two systems for the complete latitude band, this would place the balloon-borne observations on the left side of the satellite instruments, suggesting severe positive biases for all three satellite data sets. Above 50 hPa, the situation is reversed, with FIRS-2 showing large positive deviations to ACE-FTS and therefore even larger differences to MIPAS and HIRDLS. The fact that the balloon-borne measurements in the MS are larger than the satellite instruments is consistent for all analyzed latitude bands and also apparent for CFC-11. However, the high-latitude comparison for CFC-12 reveals the largest disagreement, indicating that the individual profiles might show substantial deviations from the zonal mean values in this region of high variability. In addition the FIRS-2 measurements show very large uncertainties above 50 hPa of up to 100 % (Mahieu et al., 2008).

4.2 Temporal variations in the differences

Temporal variations in CFC-12 distributions are dominated by seasonal and interannual variability. In the tropics (Supplement Fig. S12), MIPAS and HIRDLS CFC-12 time se-

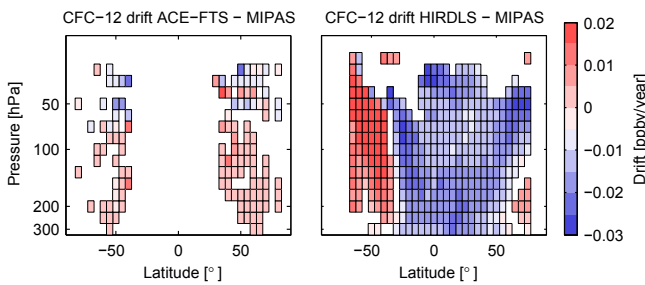


Figure 7. Altitude–latitude cross sections of drifts between ACE-FTS and MIPAS (left panel) and HIRDLS and MIPAS (right panel) CFC-12 climatologies are given in form of the linear terms [ppbv year^{-1}] derived from multi-linear regression of the difference time series.

ries show an approximately 2-year-long cycle related to the QBO transport variations. ACE-FTS measurements do not clearly reveal the same cycle, which might be related to higher uncertainties near the top of the vertical range. In the tropical UT, MIPAS data show an offset separating the data before and after January 2005, which is explained by the two different measurement modes the instrument was operating in during these time periods. At high latitudes (Supplement Fig. S13), the dominant signal is the seasonal cycle with a minimum in late winter/early spring and a maximum in late summer related to the diabatic descent of aged air within the BDC. HIRDLS and MIPAS show approximately the same seasonal cycle, with the largest disagreement at the end of the HIRDLS measurement time period in autumn 2007, where HIRDLS shows a decline in CFC-12 values that begins 3 months earlier than in MIPAS. ACE-FTS measurements do not allow for a detailed analysis of the seasonal signal, but it becomes clear that there is no pronounced minimum in late winter in the ACE-FTS time series. Interannual anomalies are quite small for all data sets (between 5 and 20 % of the absolute values) and peak in late winter/early spring with good agreement between MIPAS and HIRDLS.

In addition to seasonal and interannual variations, the time series can differ in their long-term changes due to drifts between the instruments. Figure 7 shows the drifts between ACE-FTS and MIPAS (left panel) and HIRDLS and MIPAS (right panel) CFC-12 climatologies in the form of the linear terms [ppbv year^{-1}] derived from the regression of the difference time series. Only significant linear trend terms (with $p < 0.05$ assuming normally distributed uncorrelated residuals) based on difference time series with more than 15 data points are displayed. For ACE-FTS, the linear drift terms are only significant in the mid-latitudes similar to CFC-11. The drift terms are positive and relatively small (up to $0.015 \text{ ppbv year}^{-1}$), indicating a slow, positive drift between ACE-FTS and MIPAS. For HIRDLS, the linear terms change sign with latitude, giving an inconsistent picture with positive drifts between HIRDLS and MIPAS only south of 40° S . As mentioned before, the linear drift term between HIRDLS and

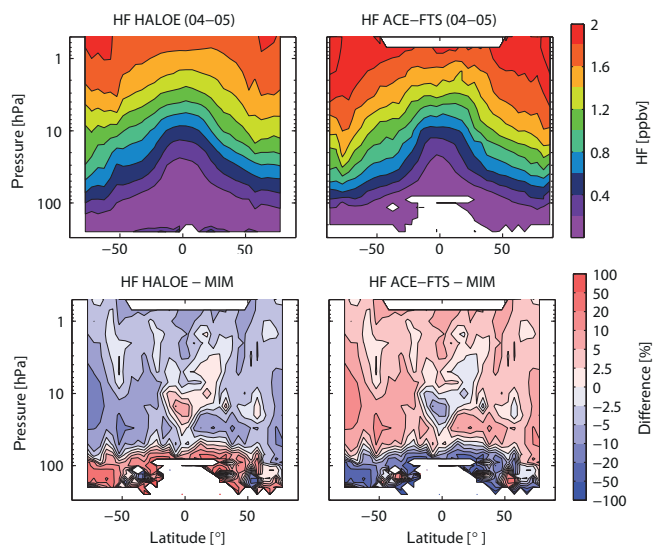


Figure 8. Altitude–latitude cross sections of annual zonal mean HF (upper panels) for HALOE and ACE-FTS and relative differences between the individual instruments and the MIM (lower panels) are shown for 2004–2005.

MIPAS is based on a 3-year-long time series only and could therefore be related to different representations of annual or multi-year oscillations.

5 Evaluation of the HF climatologies

5.1 Spatial structure of the differences

Figure 8 shows the annual zonal mean HF climatologies for 2004–2005 for HALOE and ACE-FTS. HF increases with altitude due to the combination of its stratospheric source (the photolysis of CFCs, HCFCs, and HFCs) and a very long lifetime. The HF isopleths slope downwards towards higher latitudes as a result of tropical upwelling and extratropical downwelling within the BDC. The annual mean HF distributions observed by HALOE and ACE-FTS show the same overall shape. HALOE isopleths display some kinks at $50\text{--}60^\circ \text{ S}$ and $50\text{--}60^\circ \text{ N}$ which are, at least partially, related to the HALOE sampling pattern. The change in the latitudinal coverage from month to month can cause such discontinuities. Note that HALOE coverage was reduced after 2002. Similar kinks can be observed in the ACE-FTS isopleths at around 80° S .

The relative differences of HALOE and ACE-FTS annual means to the MIM are displayed in Fig. 8. Above 50 hPa (10 hPa at the Equator), HALOE detects less HF than ACE-FTS with differences to their mean of mostly up to $\pm 5\%$ and in some areas up to $\pm 10\%$. The only exception to the good agreement are the SH high latitudes, where differences between the annual mean climatologies can become as large as 40 % (corresponding to differences to their MIM of $\pm 20\%$). The fact that HALOE observes less HF than

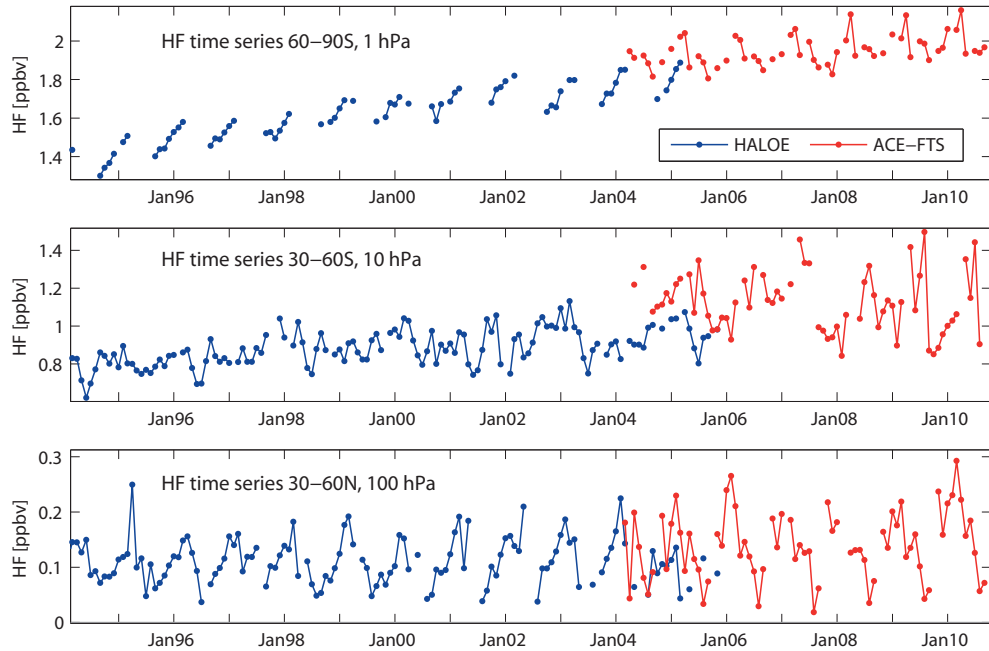


Figure 9. Time series of HF monthly mean values for 60–90° S at 1 hPa (upper panel), 30–60° S at 10 hPa (middle panel), and 30–60° N at 100 hPa (lower panel).

ACE-FTS in the MS/US is consistent with existing comparisons of HALOE to other instruments such as ATMOS with differences ranging from 10 to 40 % (Russell III et al., 1996). Independent balloon-borne observations, on the other hand, show lower values than ACE-FTS with deviations in the range 10–20 % (non-coincident profile comparisons with Mark-IV) and of 20–40 % (coincident profile comparisons with FIRS-2) (Mahieu et al., 2008). The UTLS and the tropical MS are the only regions where ACE-FTS measures less HF than HALOE with differences to their MIM mostly below ± 10 % but in some parts of the UT exceeding ± 50 %. Note that HF mixing ratios are comparably small in the UT (less than 0.2 ppbv) and therefore the absolute differences are not very large. For each individual latitude band, the two instruments measure during different months, impacting the representativeness of the annual mean differences. In particular, the high-latitude climatologies will be influenced by the different sampling of the vortex. At other latitudes, however, the annual mean differences give a picture which is in general consistent with monthly mean differences (see Supplement Figs. S14–S17 for January, April, July and September).

5.2 Temporal variations in the differences

The two HF time series from HALOE and ACE-FTS overlap only for 2 years, which makes a quantitative comparison of the seasonal cycle and interannual variability difficult. Figure 9 shows the time series of monthly mean values from 1994 to 2010 for SH high latitudes at 1 hPa and SH (NH) mid-latitudes at 10 hPa (100 hPa). The three case studies have

been chosen to illustrate the different timescales of variability that dominate at the different altitude levels. In the US at SH high latitudes, both time series show increasing values over their respective lifetimes, indicating a positive trend as the dominant signal. A seasonal cycle with increasing HF abundance over the summer is apparent in the HALOE time series and is also found for ACE-FTS. In the NH mid-latitude region at 10 hPa, the signal of interannual variability dominates both time series, with stronger variations in the later time period of the ACE-FTS record. In the NH mid-latitude LS, the seasonal cycle is the strongest signal and both time series agree on its overall shape with maximum values in the winter. A more detailed comparison of the overlap period, however, shows stronger month-to-month variations in ACE-FTS and therefore considerable disagreement of 50 to 200 % between the two time series for individual months.

6 Evaluation of the SF₆ climatologies

6.1 Spatial structure of the differences

Figure 10 shows the annual zonal mean SF₆ climatologies for 2005–2010 from MIPAS and ACE-FTS. SF₆ decreases with increasing altitude due to the combination of its very long lifetime, growing tropospheric emissions, and stratospheric transport timescales. The SF₆ isopleths slope downwards towards higher latitudes as a result of air mass transport within the BDC. While MIPAS and ACE-FTS observe an overall similar annual mean SF₆ distribution, some clear differences exist. ACE-FTS shows much noisier isopleths very likely as

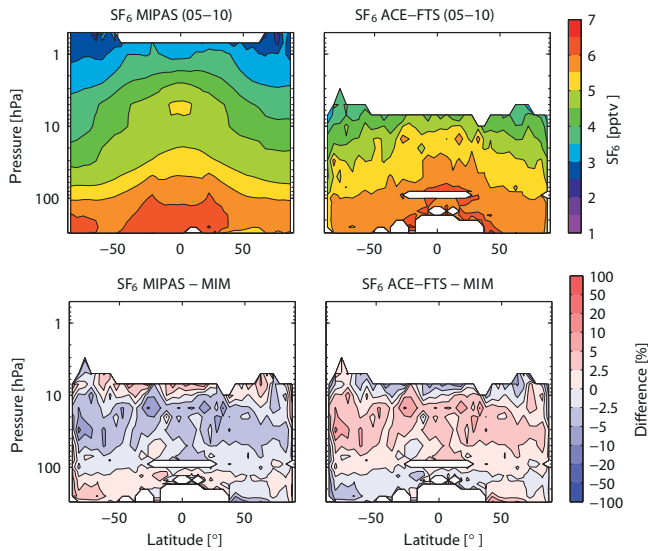


Figure 10. Altitude–latitude cross sections of annual zonal mean SF₆ (upper panels) for MIPAS and ACE-FTS and relative differences between the individual instruments and the MIM (lower panels) are shown for 2005–2010.

result of its less dense sampling. Apart from the noisy structure with several kinks, ACE-FTS isopleths, in particular the ones around 4.5 pptv, are less steep than the corresponding MIPAS isopleths. This is possibly related to the relatively low maximum retrieval altitude of ACE-FTS. Another notable feature is the peaks of MIPAS SF₆ in the UTLS (i.e., at the 5.5 and 6 pptv isopleths) around 25° S/25° N. These mixing ratio peaks are visible in the annual mean climatologies; however, monthly mean evaluations (see Supplement Figs. S18–S21 for January, April, July and October) demonstrate that they are most pronounced in the respective winter/spring hemisphere. The phenomenon is also apparent in the MIPAS CFC-12 and, to a smaller degree, CFC-11 latitudinal profiles in the UTLS with the same seasonal dependence. Note that these peaks do not exist in ACE-FTS or HIRDLS data for any of the three gases; however, a straightforward comparison is hampered by the less dense sampling of ACE-FTS and the tropical data gaps in HIRDLS. The enhanced mixing ratios at 25° in the winter/spring hemisphere, as observed by MIPAS, are possibly related to the seasonality of mixing and upwelling in the tropical UTLS and indicate younger air in this region (Stiller et al., 2012). Additionally, the effect could be intensified by temperature artifacts.

In spite of the somewhat differently shaped SF₆ isopleths of MIPAS and ACE-FTS discussed above, the instruments show overall very good agreement. Relative differences to their MIM are often below $\pm 2.5\%$ (Fig. 10, lower panels). Only around 50 to 10 hPa are the differences slightly larger, occasionally reaching $\pm 10\%$. At altitudes below 100 hPa, MIPAS detects larger SF₆ abundances, while above 100 hPa

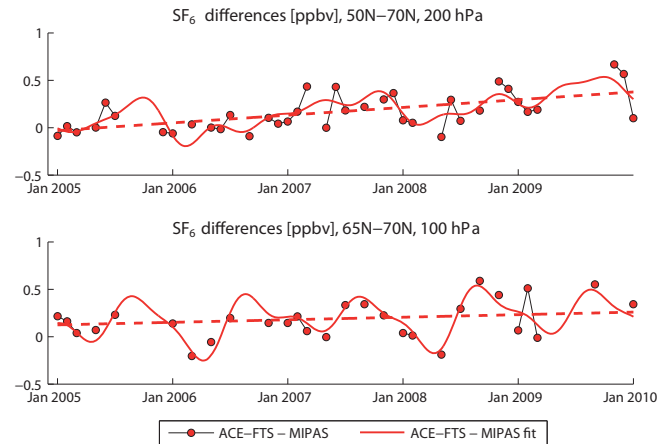


Figure 11. Time series of zonal monthly mean SF₆ absolute differences between ACE-FTS and MIPAS (black lines, red symbols) are given for 2005 to 2010 at 50–70° N on 200 and at 65–70° N at 100 hPa. Additionally, the calculated fit (solid colored line) and the corresponding linear term (dashed colored line) are shown.

ACE-FTS does not decrease as fast as MIPAS and shows larger values.

6.2 Temporal variations in the differences

Temporal variations in the SF₆ time series are dominated by long-term changes caused by increasing tropospheric emissions and changes in atmospheric transport. Exceptions to this are found at high latitudes, where SF₆ shows a pronounced seasonal cycle with minima in spring related to descending air which might have experienced chemical loss of SF₆ in the mesosphere (Stiller et al., 2008). While MIPAS data clearly display this seasonal signal in the SH polar latitudes, the ACE-FTS time series is more noisy with larger month-to-month fluctuations but also indicates reduced SF₆ abundance in spring (not shown here; see SPARC Data Initiative report for details).

A multiple linear regression, as described for CFC-11 in Sect. 3.2, has been carried out in order to analyze the long-term change in the differences. For nearly all latitudes and altitudes the time series of the differences between ACE-FTS and MIPAS are dominated by short-term variability and have no statistically significant linear trend term. The only exception to this is the NH high latitudes (50–70° N) between 200 and 100 hPa. As an example, Fig. 11 shows the absolute difference time series at 200 and 100 hPa together with the fit derived from the multi-linear regression and the linear trend term of the fit. Both difference time series indicate a positive drift of ACE-FTS with respect to MIPAS in this atmospheric region of 0.08 and 0.03 pptv year⁻¹, respectively.

7 Summary and discussion

A comprehensive comparison of CFC-11, CFC-12, HF and SF₆ profile climatologies from four satellite instruments has been carried out. An uncertainty estimate in our knowledge of the atmospheric mean state is derived from the spread between the data sets and presented in Fig. 12. The annual zonal MIMs of all four gases are presented for the respective main evaluation periods. The spread between the instrumental climatologies is given by the standard deviation over all instruments presented in absolute and relative values to provide a measure of the uncertainty in the underlying field. The derived overall findings on the systematic uncertainty in our knowledge of the atmospheric mean state, as given by the satellite data sets, are presented in the following summary together with important characteristics of the individual data sets. Information from other in situ, ground- or balloon-based remote measurements cannot be included in the uncertainty estimates in a systematic way due to their sparseness. Cases where validation studies suggest that the satellite-derived uncertainty could be only a lower estimate (i.e., differences to in situ measurements are larger than among the satellite data sets) are discussed. Note, however, that for such a discussion important assumptions have to be made and coincident profile comparisons have to be considered representative of instrument biases over complete latitude bands. As a consequence, uncertainty estimates derived from coincident profile comparisons have to be considered with care, while the uncertainty estimates derived from the spread among the satellite data sets are global results much less impacted by geo-physical variability.

7.1 Summary for CFC-11 and CFC-12

CFC-11 and CFC-12 vertically resolved climatologies are available from three satellite instruments, MIPAS, ACE-FTS and HIRDLS, which overlap in 2005–2007.

The uncertainty in our knowledge of the atmospheric CFC-11 annual mean state is small at altitudes below 100 hPa with a 1σ multi-instrument spread of less than $\pm 5\%$ in the tropics and mid-latitudes and less than $\pm 10\%$ at higher latitudes for the 2005–2007 period. Maximum CFC-11 mixing ratios in the tropical TTL with values up to 0.275 ppbv are larger than those measured near the surface (0.26 ppbv) suggesting a bias of up to 5 %. While the satellite CFC-11 mixing ratios in the tropics potentially have a positive bias, coincident profile comparisons to independent data at the mid-latitudes suggest that the satellite instruments could be too low (5 to 10 %). If this offset were valid for the whole latitude band, this would increase the uncertainty in our knowledge of the atmospheric CFC-11 annual mean state at altitudes below 100 hPa from 5 to 10 %.

In the tropical LS, the spread between the data sets increases quickly with increasing altitude from $\pm 5\%$ (at 50 hPa) to $\pm 30\%$ (at 30 hPa). Here, the absolute differences

between the data sets are largest with deviations between 0.15 and 0.25 ppb due to high ACE-FTS values. In the mid- and high-latitude LS between 100 and 70 hPa, absolute deviations increase slightly, resulting in a spread of $\pm 10\%$. At high latitudes, coincident profile comparisons to balloon-borne measurements suggest a negative bias of all three data sets, which, if assumed to be a general feature and not just a local exception or a bias of the balloon-borne measurements, would increase the uncertainty in our knowledge of the atmospheric CFC-11 annual mean state to $\pm 15\%$. Above 70 hPa, a large relative spread of up to $\pm 50\%$ exists for very low background values (0.05 ppb).

The uncertainty in our knowledge of the atmospheric CFC-12 annual mean state is very small at altitudes below 100 hPa (see Fig. 12). The evaluation of three data sets for the time period 2005–2007 reveals a 1σ multi-instrument spread in this region of less than $\pm 5\%$ and often even less than $\pm 2.5\%$. This very small uncertainty is confirmed by balloon-borne measurements in the mid-latitudes. Only at the high NH latitudes do independent data sets suggest a positive bias of the satellite instruments which would increase the uncertainty in our knowledge of the atmospheric CFC-12 mean state to $\pm 15\%$. The satellite data sets show maximum CFC-12 mixing ratios of 0.6 ppbv in the TTL, indicating a high bias of up to 5 %. In the region between 100 and 20 hPa, good agreement between all data sets exists in the tropics, in the NH, and in the SH subtropics with a multi-instrument spread of less than $\pm 10\%$. Deviations to independent profile data sets are largest at the NH high latitudes possibly impacted by sampling effects in a region of high spatial variability.

Overall, there is a better agreement of the CFC-12 climatologies than of the CFC-11 climatologies, in particular between 70 and 30 hPa. Discrepancies in the performance in the NH and SH extratropical regions exist mostly for CFC-12, where a large inter-instrument spread is found in the SH above 50 hPa. However, for CFC-11 the vertical range extends only to 30 hPa, making it more difficult to detect such hemispheric differences reliably.

A large number of instrument-specific features can be observed for both tracers. MIPAS CFC-11 and CFC-12 in the winter hemisphere have different meridional gradients at 200 hPa than the other two instruments. ACE-FTS has problems at its highest retrieval level in the tropics for both tracers, but this is more pronounced for CFC-11. In addition to the unrealistic elevated values at the highest retrieval level, ACE-FTS shows in most regions no clear signals of seasonal cycle or interannual variability, which might be partially related to the low data sampling. HIRDLS climatologies of CFC-11 and CFC-12 both show steeper gradients in the subtropics, large negative deviations in the mid-latitudes and an earlier decline in the seasonal cycle in late 2007.

Finally, there are some instrument-specific features which differ considerably between the two CFCs. One example is the seasonal cycle at NH high latitudes, which ACE-FTS can detect for CFC-11 but not for CFC-12. The difference time

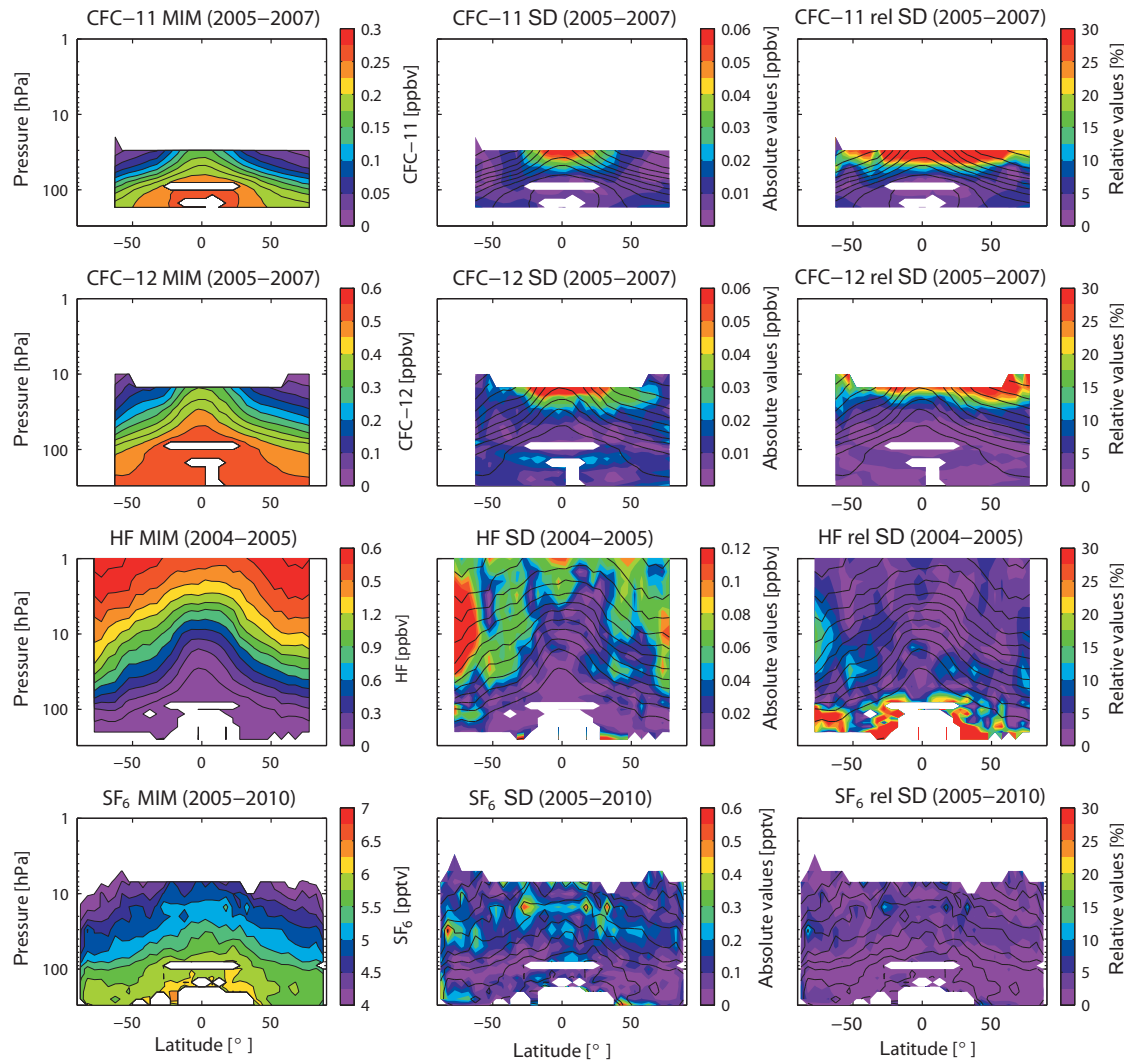


Figure 12. Summary of CFC-11, CFC-12, HF and SF_6 annual zonal mean state for the respective evaluation period. Annual zonal mean cross sections of the MIM of each trace gas are shown in the left panel. Additionally, the standard deviations (SD) over all respective instruments are presented in the middle panel. Relative standard deviations (calculated by dividing the absolute standard deviation by the MIM) are shown in the right panels. Black contour lines in the middle and right panels give the MIM distribution. Instruments included are MIPAS, ACE-FTS, and HIRDLS for CFC-11, CFC-12, HALOE and ACE-FTS for HF, and MIPAS, and ACE-FTS for SF_6 . The MIM and standard deviation are only displayed for regions where all instruments provide measurements.

series of ACE-FTS with respect to MIPAS shows a positive drift in the extratropics for CFC-11 and to a smaller degree also for CFC-12. The absolute difference time series of HIRDLS and MIPAS includes also a statistically significant linear component; however, due to the shortness of the time series this component might be related to different representations of annual or multi-year oscillations. Nevertheless, for CFC-11, the HIRDLS-MIPAS comparison yields the same drift behavior in the NH lower stratosphere as the ACE-MIPAS comparison, suggesting that the drift is related to issues in the MIPAS record. Given the magnitude of the drift (which, in this region, is up to 0.02 ppbv or 10 % over the considered time period of 6 years), trends derived from the

different data sets need to undergo further evaluation before conclusions can be drawn.

7.2 Summary for HF and SF_6

Vertically resolved HF climatologies are available from HALOE and ACE-FTS, which overlap in 2004–2005. The uncertainty in our knowledge of the atmospheric HF annual mean state as derived from the two satellite data sets and shown in Fig. 12 is smallest above 100 hPa, with a 1σ multi-instrument spread in this region of less than $\pm 10\%$ ($\pm 5\%$ above 10 hPa). One exception is the SH high latitudes where the two annual mean climatologies give a spread of $\pm 15\%$

in the MS. The larger disagreement in the SH high latitudes is mainly caused by the fact that the annual mean data sets for both instruments are impacted by sampling biases. The evaluation of individual monthly mean profiles shows that differences in the NH and SH high latitudes are of the same magnitude compared to differences at lower latitudes. At altitudes below 100 hPa the HF annual mean state is less well known, with a 1σ multi-instrument spread in this region of $\pm 30\%$ and larger. Analysis of the seasonal cycle and interannual anomalies reveals that merging exercises of the two time series would be straightforward at the upper levels where differences are about 10 % and quite consistent during the overlap time period. Merging of HALOE and ACE-FTS HF in the LS, however, would be more complicated since the mean differences can be large (50 to 200 %) for individual months.

Vertically resolved SF₆ climatologies are available from MIPAS and ACE-FTS, which overlap during 2005–2010. The uncertainty in our knowledge of the atmospheric SF₆ annual mean state as derived from the two satellite data sets is very small, with a sigma multi-instrument spread of less than $\pm 5\%$ and often below $\pm 2.5\%$. MIPAS SF₆ in the UTLS around 25° S/25° N shows some elevated mixing ratio peaks, which are most pronounced in the respective winter/spring hemisphere. In addition to SF₆, the phenomenon is also apparent in the MIPAS CFC-12 and, to a smaller degree, CFC-11 latitudinal profiles in the UTLS with the same seasonal dependence. Another feature that can be observed for all three gases is the fact that mixing ratios derived by ACE-FTS do not decrease as fast as the comparison instruments with increasing altitude in the MS. The time series of the differences between SF₆ ACE-FTS and MIPAS are dominated by short-term variability and show no significant linear drift. The only exception to this is the NH high latitudes (50–70° N) between 200 and 100 hPa, where a positive drift of ACE-FTS with respect to MIPAS exists.

The Supplement related to this article is available online at doi:10.5194/essd-8-61-2016-supplement.

Acknowledgements. These climatological comparisons have resulted from the extensive work of the SPARC Data Initiative team since 2009. The authors thank the relevant instrument teams, the various space agencies (CSA, ESA, NASA, JAXA), and organizations such as CEOS-ACC and IGACO. We particularly thank the ISSI in Bern for facilitating two successful team meetings in Bern as part of the ISSI International Team activity program and SPARC and WCRP for travel support. The work from S. Tegtmeier was funded from the EU project SHIVA (FP7-ENV-2007-1-226224) and the BMBF ROMIC grant THREAT 01LG1217A. M. I. Hegglin thanks the CSA and ESA for supporting her work for the SPARC Data Initiative. ACE is a Canadian-led mission mainly supported by the CSA. Development of the ACE-FTS climatologies was supported by grants from the Canadian Foundation for Climate

and Atmospheric Sciences and the CSA. Work on the HIRDLS data was funded by NASA under contract NAS5-97046. The work from Hampton University was partially funded under the National Oceanic and Atmospheric Administration's Educational Partnership Program Cooperative Remote Sensing Science and Technology Center (NOAA EPP CREST).

The article processing charges for this open-access publication were covered by a Research Centre of the Helmholtz Association.

Edited by: G. König-Langlo

References

Austin, J. and Li, F.: On the relationship between the strength of the Brewer-Dobson circulation and the age of stratospheric air, *Geophys. Res. Lett.*, 33, L17807, doi:10.1029/2006GL026867, 2006.

Brown, A. T., Chipperfield, M. P., Boone, C., Wilson, C., Walker, K. A., and Bernath, P. F.: Trends in atmospheric halogen containing gases since 2004, *J. Quant. Spectrosc. Ra.*, 112, 2552–2566, doi:10.1016/j.jqsrt.2011.07.005, 2011.

Bujok, O., Tan, V., Klein, E., Nopper, R., Bauer, R., Engel, A., Gerhards, M.-T., Afchine, A., McKenna, D. S., Schmidt, U., Wienhold, F. G., and Fischer, H.: GHOST – a novel airborne gas chromatograph for in situ measurements of long-lived tracers in the lower stratosphere: Method and Applications, *J. Atmos. Chem.*, 39, 37–64, 2001.

Butchart, N., Scaife, A. A., Bourqui, M., de Grandpré, J., Hare, S. H. E., Kettleborough, J., Langematz, U., Manzini, E., Sassi, F., Shibata, K., Shindell, D., and Sigmond, M.: Simulations of anthropogenic change in the strength of the Brewer–Dobson circulation, *Clim. Dynam.*, 27, 727–741, 2006.

Daniel, J. S., Velders, G. J. M., Solomon, S., McFarland, M., and Montzka, S. A.: Present and future sources and emissions of halocarbons: Toward new constraints, *J. Geophys. Res.*, 112, D02301, doi:10.1029/2006JD007275, 2007.

Eckert, E., von Clarmann, T., Kiefer, M., Stiller, G. P., Lossow, S., Glatthor, N., Degenstein, D. A., Froidevaux, L., Godin-Beekmann, S., Leblanc, T., McDermid, S., Pastel, M., Steinbrecht, W., Swart, D. P. J., Walker, K. A., and Bernath, P. F.: Drift-corrected trends and periodic variations in MIPAS IMK/IAA ozone measurements, *Atmos. Chem. Phys.*, 14, 2571–2589, doi:10.5194/acp-14-2571-2014, 2014.

Eckert, E., Laeng, A., Lossow, S., Kellmann, S., Stiller, G., von Clarmann, T., Glatthor, N., Höpfner, M., Kiefer, M., Oelhaf, H., Orphal, J., Funke, B., Grabowski, U., Haenel, F., Linden, A., Wetzel, G., Woiwode, W., Bernath, P. F., Boone, C., Dutton, G. S., Elkins, J. W., Engel, A., Gille, J. C., Kolonjari, F., Sugita, T., Toon, G. C., and Walker, K. A.: MIPAS IMK/IAA CFC-11 (CCl₃F) and CFC-12 (CCl₂F₂) measurements: accuracy, precision and long-term stability, *Atmos. Meas. Tech. Discuss.*, 8, 7573–7662, doi:10.5194/amt-8-7573-2015, 2015.

Elkins, J. W., Fahey, D. W., Gilligan, J. M., Dutton, G. S., Barling, T. J., Volk, C. M., Dunn, R. E., Myers, R. C., Montzka, S. A., Wamsley, P. R., Hayden, A. H., Butler, J. H., Thompson, T. M., Swanson, T. H., Slugokenky, E. J., Novelli, P.

C., Hurst, D. F., Lobert, J. M., Ciciora, S. J., McLaughlin, R. J., Thompson, T. L., Winkler, R. H., Fraser, P. J., Steele, L. P., and Lucarelli, M. P.: Airborne gas chromatograph for in situ measurements of long-lived species in the upper troposphere and lower stratosphere, *Geophys. Res. Lett.*, 23, 347–350, doi:10.1029/96GL00244, 1996.

Engel, A., Schmidt, U., and McKenna, D.: Stratospheric trends of CFC-12 over the past two decades: Recent observational evidence of declining growth rates, *Geophys. Res. Lett.*, 25, 3319–3322, 1998.

Engel, A., Bönisch, H., Brunner, D., Fischer, H., Franke, H., Günther, G., Gürk, C., Hegglin, M., Hoor, P., Königstedt, R., Krebsbach, M., Maser, R., Parchatka, U., Peter, T., Schell, D., Schiller, C., Schmidt, U., Spelten, N., Szabo, T., Weers, U., Wernli, H., Wetter, T., and Wirth, V.: Highly resolved observations of trace gases in the lowermost stratosphere and upper troposphere from the Spurt project: an overview, *Atmos. Chem. Phys.*, 6, 283–301, doi:10.5194/acp-6-283-2006, 2006.

Funke, B. and von Clarmann, T.: How to average logarithmic retrievals?, *Atmos. Meas. Tech.*, 5, 831–841, doi:10.5194/amt-5-831-2012, 2012.

Gille, J., Gray, L., Cavanaugh, C., Coffey, M., Dean, V., Halvorsen, C., Karol, S., Khosravi, R., Kinnison, D., Massie, S., Nardi, B., Belmonte Rivas, M., Smith, L., Torpy, B., Waterfall, A., and Wright, C.: High Resolution Dynamics Limb Sounder Earth Observing System (EOS) Data description and quality, Version 7 (V7), http://www.eos.ucar.edu/hirdls/data/products/HIRDLS-DQD_V7-1.pdf (last access: 27 March 2015), 2013.

Groß, J.-U. and Russell III, James M.: Technical note: A stratospheric climatology for O₃, H₂O, CH₄, NO_x, HCl and HF derived from HALOE measurements, *Atmos. Chem. Phys.*, 5, 2797–2807, doi:10.5194/acp-5-2797-2005, 2005.

Haenel, F. J., Stiller, G. P., von Clarmann, T., Funke, B., Eckert, E., Glatthor, N., Grabowski, U., Kellmann, S., Kiefer, M., Linden, A., and Reddmann, T.: Reassessment of MIPAS age of air trends and variability, *Atmos. Chem. Phys.*, 15, 13161–13176, doi:10.5194/acp-15-13161-2015, 2015.

Hall, T. M. and Plumb, R. A.: Age as a diagnostic of stratospheric transport, *J. Geophys. Res.*, 99, 1059–1070, doi:10.1029/93JD03192, 1994.

Hegglin, M. I., Tegtmeier, S., Anderson, J., Froidevaux, L., Fuller, R., Funke, B., Jones, A., Lingenfelter, G., Lumpe, J., Pendlebury, D., Remsberg, E., Rozanov, A., Toohey, M., Urban, J., von Clarmann, T., Walker, K. A., Wang, R., and Weigel, K.: SPARC Data Initiative: Comparison of water vapor climatologies from international satellite limb sounders, *J. Geophys. Res.-Atmos.*, 118, 11824–11846, doi:10.1002/jgrd.50752, 2013.

Hoffmann, L., Kaufmann, M., Spang, R., Müller, R., Remedios, J. J., Moore, D. P., Volk, C. M., von Clarmann, T., and Riese, M.: Envisat MIPAS measurements of CFC-11: retrieval, validation, and climatology, *Atmos. Chem. Phys.*, 8, 3671–3688, doi:10.5194/acp-8-3671-2008, 2008.

Johnson, D. G., Jucks, K. W., Traub, W. A., and Chance, K. V.: Smithsonian stratospheric far-infrared spectrometer and data reduction system, *J. Geophys. Res.*, 100, 2091–3106, 1995.

Jones, A., Qin, G., Strong, K., Walker, K. A., McLinden, C. A., Toohey, M., Kerzenmacher, T., Bernath, P. F., and Boone, C. D.: A global inventory of stratospheric NO_y from ACE-FTS, *J. Geophys. Res.*, 116, D17304, doi:10.1029/2010JD015465, 2011.

Jones, A., Walker, K. A., Jin, J. J., Taylor, J. R., Boone, C. D., Bernath, P. F., Brohede, S., Manney, G. L., McLeod, S., Hughes, R., and Daffer, W. H.: Technical Note: A trace gas climatology derived from the Atmospheric Chemistry Experiment Fourier Transform Spectrometer (ACE-FTS) data set, *Atmos. Chem. Phys.*, 12, 5207–5220, doi:10.5194/acp-12-5207-2012, 2012.

Kellmann, S., von Clarmann, T., Stiller, G. P., Eckert, E., Glatthor, N., Höpfner, M., Kiefer, M., Orphal, J., Funke, B., Grabowski, U., Linden, A., Dutton, G. S., and Elkins, J. W.: Global CFC-11 (CCl₃F) and CFC-12 (CCl₂F₂) measurements with the Michelson Interferometer for Passive Atmospheric Sounding (MIPAS): retrieval, climatologies and trends, *Atmos. Chem. Phys.*, 12, 11857–11875, doi:10.5194/acp-12-11857-2012, 2012.

Ko, M. K. W., Sze, N. D., Wang, W.-C., Shia, G., Goldman, A., Murcray, F. J., Murcray, D. G., and Rinsland, C. P.: Atmospheric sulfur hexafluoride: Sources, sinks and greenhouse warming, *J. Geophys. Res.*, 98, 10499–10507, doi:10.1029/93JD00228, 1993.

Kohlhepp, R., Ruhnke, R., Chipperfield, M. P., De Mazière, M., Notholt, J., Barthlott, S., Batchelor, R. L., Blatherwick, R. D., Blumenstock, Th., Coffey, M. T., Demoulin, P., Fast, H., Feng, W., Goldman, A., Griffith, D. W. T., Hamann, K., Hannigan, J. W., Hase, F., Jones, N. B., Kagawa, A., Kaiser, I., Kasai, Y., Kirner, O., Kouker, W., Lindenmaier, R., Mahieu, E., Mittermeier, R. L., Monge-Sanz, B., Morino, I., Murata, I., Nakajima, H., Palm, M., Paton-Walsh, C., Raffalski, U., Reddmann, Th., Rettinger, M., Rinsland, C. P., Rozanov, E., Schneider, M., Senten, C., Servais, C., Sinnhuber, B.-M., Smale, D., Strong, K., Sussmann, R., Taylor, J. R., Vanhaevelyn, G., Warneke, T., Whalley, C., Wiegle, M., and Wood, S. W.: Observed and simulated time evolution of HCl, ClONO₂, and HF total column abundances, *Atmos. Chem. Phys.*, 12, 3527–3556, doi:10.5194/acp-12-3527-2012, 2012.

Levin, I., Naegler, T., Heinz, R., Osusko, D., Cuevas, E., Engel, A., Ilmberger, J., Langenfelds, R. L., Neininger, B., Rohden, C. v., Steele, L. P., Weller, R., Worthy, D. E., and Zimov, S. A.: The global SF₆ source inferred from long-term high precision atmospheric measurements and its comparison with emission inventories, *Atmos. Chem. Phys.*, 10, 2655–2662, doi:10.5194/acp-10-2655-2010, 2010.

Luo, M., Cicerone, R. J., and Russell III, J. M.: Analysis of Halogen Occultation Experiment HF versus CH₄ correlation plots: Chemistry and transport implications, *J. Geophys. Res.*, 100, 13927–13937, doi:10.1029/95JD00621, 1995.

Mahieu, E., Duchatelet, P., Demoulin, P., Walker, K. A., Dupuy, E., Froidevaux, L., Randall, C., Catoire, V., Strong, K., Boone, C. D., Bernath, P. F., Blavier, J.-F., Blumenstock, T., Coffey, M., De Mazière, M., Griffith, D., Hannigan, J., Hase, F., Jones, N., Jucks, K. W., Kagawa, A., Kasai, Y., Mebarki, Y., Mikuteit, S., Nassar, R., Notholt, J., Rinsland, C. P., Robert, C., Schrems, O., Senten, C., Smale, D., Taylor, J., Tétard, C., Toon, G. C., Warneke, T., Wood, S. W., Zander, R., and Servais, C.: Validation of ACE-FTS v2.2 measurements of HCl, HF, CCl₃F and CCl₂F₂ using space-, balloon- and ground-based instrument observations, *Atmos. Chem. Phys.*, 8, 6199–6221, doi:10.5194/acp-8-6199-2008, 2008.

Molina M. J. and Rowland F. S.: Stratospheric sink for chlorofluoromethanes: Chlorine-atom catalyzed destruction of ozone, *Nature*, 249, 810–814, 1974.

Montzka, S. and Reimann, S.: Ozone-depleting substances (ODSs) and related chemicals, in Scientific Assessment of Ozone Depletion: 2010, Rep. 52, chap. 1, Global Ozone Res. and Monit. Proj., World Meteorol. Organ., Geneva, Switzerland, 1–112, 2011.

Morris, R. A., Miller, T. M., Viggiano, A. A., Paulson, J. F., Solomon, S., and Reid, G.: Effects of electron and ion reactions on atmospheric lifetimes of fully fluorinated compounds, *J. Geophys. Res.*, 100, 1287–1294, doi:10.1029/94JD02399, 1995.

Neu, J. L., Hegglin, M. I., Tegtmeier, S., Bourassa, A., Degenstein, D., Froidevaux, L., Fuller, R., Funke, B., Gille, J., Jones, A., Rozanov, A., Toohey, M., von Clarmann, T., Walker, K. A., and Worden, J. R.: The SPARC Data Initiative: Comparison of upper troposphere/lower stratosphere ozone climatologies from limb-viewing instruments and the nadir-viewing Tropospheric Emission Spectrometer, *J. Geophys. Res.-Atmos.*, 119, 6971–6990, doi:10.1002/2013JD020822, 2014.

Ravishankara, A. R., Solomon, S., Turnipseed, A. A., and Warren, R. F.: Atmospheric lifetimes of long-lived halogenated species, *Science*, 259, 194–199, doi:10.1126/science.259.5092.194, 1993.

Reddmann, T., Ruhnke, R., and Kouker, W.: Three-dimensional model simulations of SF₆ with mesospheric chemistry, *J. Geophys. Res.*, 106, 14525–14537, doi:10.1029/2000JD900700, 2001.

Rinsland, C. P., Gunson, M. R., Abrams, M. C., Lowes, L. L., Zander, R., and Mahieu, E.: ATMOS/ATLAS 1 measurements of sulfur hexafluoride (SF₆) in the lower stratosphere and upper troposphere, *J. Geophys. Res.*, 98, 20491–20494, doi:10.1029/93JD02258, 1993.

Rinsland, C. P., Boone, C., Nassar, R., Walker, K., Bernath, P., Mahieu, E., Zander, R., McConnell, J. C., and Chiou, L.: Trends of HF, HCl, CCl₂F₂, CCl₃F, CHClF₂ (HCFC-22), and SF₆ in the lower stratosphere from Atmospheric Chemistry Experiment (ACE) and Atmospheric Trace Molecule Spectroscopy (ATMOS) measurements near 30° N latitude, *Geophys. Res. Lett.*, 32, L16S03, doi:10.1029/2005GL022415, 2005.

Russell III, J. M., Deaver, L. E., Luo, M., Park, J. H., Gordley, L. L., Tuck, A. F., Toon, G. C., Gunson, M. R., Traub, W. A., Johnson, D. G., Jucks, K. W., Murcray, D. G., Zander, R., Nolt, I. G., and Webster, C. R.: Validation of hydrogen fluoride measurements made by the Halogen Occultation Experiment from the UARS platform, *J. Geophys. Res.*, 101, 10163–10174, doi:10.1029/95JD01705, 1996.

SPARC Data Initiative: SPARC Report No. 6, edited by: Hegglin, M. and Tegtmeier, S., in preparation, 2016.

Stiller, G. P., von Clarmann, T., Höpfner, M., Glatthor, N., Grabowski, U., Kellmann, S., Kleinert, A., Linden, A., Milz, M., Reddmann, T., Steck, T., Fischer, H., Funke, B., López-Puertas, M., and Engel, A.: Global distribution of mean age of stratospheric air from MIPAS SF₆ measurements, *Atmos. Chem. Phys.*, 8, 677–695, doi:10.5194/acp-8-677-2008, 2008.

Stiller, G. P., von Clarmann, T., Haenel, F., Funke, B., Glatthor, N., Grabowski, U., Kellmann, S., Kiefer, M., Linden, A., Los-sow, S., and López-Puertas, M.: Observed temporal evolution of global mean age of stratospheric air for the 2002 to 2010 period, *Atmos. Chem. Phys.*, 12, 3311–3331, doi:10.5194/acp-12-3311-2012, 2012.

Stolarski, R. S. and Rundel, R. D.: Fluorine photochemistry in the stratosphere, *Geophys. Res. Lett.*, 2, 443–444, 1975.

Tegtmeier, S., Hegglin, M. I., Anderson, J., Bourassa, A., Brohede, S., Degenstein, D., Froidevaux, L., Fuller, R., Funke, B., Gille, J., Jones, A., Kasai, Y., Krüger, K., Kyrölä, E., Lingenfelser, G., Lumpe, J., Nardi, B., Neu, J., Pendlebury, D., Remsberg, E., Rozanov, A., Smith, L., Toohey, M., Urban, J., von Clarmann, T., Walker, K. A., and Wang, R. H. J.: SPARC Data Initiative: A comparison of ozone climatologies from international satellite limb sounders, *J. Geophys. Res.-Atmos.*, 118, 12,229–12,247, doi:10.1002/2013JD019877, 2013.

Toohey, M. and von Clarmann, T.: Climatologies from satellite measurements: the impact of orbital sampling on the standard error of the mean, *Atmos. Meas. Tech.*, 6, 937–948, doi:10.5194/amt-6-937-2013, 2013.

Toohey, M., Hegglin, M. I., Tegtmeier, S., Anderson, J., Añel, J. A., Bourassa, A., Brohede, S., Degenstein, D., Froidevaux, L., Fuller, R., Funke, B., Gille, J., Jones, A., Kasai, Y., Krüger, K., Kyrölä, E., Neu, J. L., Rozanov, A., Smith, L., Urban, J., von Clarmann, T., Walker, K. A., and Wang, R. H. J.: Characterizing sampling biases in the trace gas climatologies of the SPARC Data Initiative, *J. Geophys. Res.-Atmos.*, 118, 11847–11862, doi:10.1002/jgrd.50874, 2013.

Toon, G. C., Blavier, J.-F., Sen, B., Margitan, J. J., Webster, C. R., May, R. D., Fahey, D., Gao, R., Del Negro, L., Proffitt, M., Elkins, J., Romashkin, P. A., Hurst, D. F., Oltmans, S., Atlas, E., Schaufler, S., Flocke, F., Bui, T. P., Stimpfle, R. M., Bonne, G. P., Voss, P. B., and Cohen, R. C.: Comparison of MkIV balloon and ER-2 aircraft measurements of atmospheric trace gases, *J. Geophys. Res.*, 104, 26779–26790, doi:10.1029/1999JD900379, 1999.

Volk, C. M., Elkins, J. W., Fahey, D. W., Dutton, G. S., Gilligan, J. M., Loewenstein, M., Podolske, J. R., Chan, K. R., and Gunson, M. R.: Evaluation of source gas lifetimes from stratospheric observations, *J. Geophys. Res.*, 102, 25543–25564, doi:10.1029/97JD02215, 1997.

von Clarmann, T., Stiller, G., Grabowski, U., Eckert, E., and Orphal, J.: Technical Note: Trend estimation from irregularly sampled, correlated data, *Atmos. Chem. Phys.*, 10, 6737–6747, doi:10.5194/acp-10-6737-2010, 2010.

Zander, R., Mahieu, E., Demoulin, P., Duchatelet, P., Servais, C., Roland, G., DelBouille, L., De Mazière, M., and Rinsland, C. P.: Evolution of a dozen non-CO₂ greenhouse gases above central Europe since the mid-1980s, *Environ. Sci.*, 2, 295–303, doi:10.1080/15693430500397152, 2005.